

## Bifurcations and Chaos in the Six-Dimensional Turbulence Model of Gledzer

MAKOTO UMEKI\*

*Department of Physics, Graduate School of Science, University of Tokyo,  
7-3-1 Hongo, Bunkyo-ku, Tokyo, 113-0033 Japan*

The cascade-shell model of turbulence with six real variables originated by Gledzer is studied numerically using Mathematica 5.1. Periodic, doubly-periodic and chaotic solutions and the routes to chaos via both frequency-locking and period-doubling are found by the Poincaré plot of the first mode  $v_1$ . The circle map on the torus is well approximated by the summation of several sinusoidal functions. The dependence of the rotation number on the viscosity parameter is in accordance with that of the sine-circle map. The complicated bifurcation structure and the revival of a stable periodic solution at the smaller viscosity parameter in the present model indicates that the turbulent state may be very sensitive to the Reynolds number.

KEYWORDS: bifurcation, chaos, turbulence, shell model, Mathematica

Many of turbulent phenomena in motions of fluids are considered to be understandable by investigating ordinary differential equations which are models faithful to the Navier-Stokes (NS) equations. Recent progress of computer hardware and software, however, may still not be enough to make clear the route and the characteristics of turbulence. Another prompt way to smatter turbulence is to omit the theoretical derivation of nonlinear models, to give up the full numerical simulation and to fall back on simpler models analogous to the NS equation. In this context, the cascade-shell models by Gledzer (1973)<sup>1</sup> and its complex version (Ohkitani and Yamada (OY 1989),<sup>2</sup> so-called the GOY model; see also Frisch (1995),<sup>3</sup> Kato and Yamada (2003),<sup>4</sup> Biferale(2003)<sup>5</sup> for further references) have been studied numerically from the viewpoint of turbulence statistics. In the present investigation, the bifurcation approach is made to the Gledzer's cascade-shell model of turbulence with six real variables. Biferale *et al.* (1995)<sup>6</sup> has found the limit-cycle and torus attractors in the GOY model with a fixed viscosity along with loss of the stability of the Kolmogorov 1941 fixed point when the parameter  $\epsilon$  related to the *helicity* exceeds critical values about 0.386 and 0.396, respectively. In contrast with the bifurcation found by Biferale *et al.* (1995)<sup>6</sup> in GOY interpreted as the Ruelle-Takens scenario, a detailed study of the circle map in the Gledzer model in this paper indicates that the bifurcation of torus attractors is in accordance with that of the sine-circle map. Another similar study of the five-mode truncation model of the NS equation is made by Franceschini

---

\*E-mail address: umeki@phys.s.u-tokyo.ac.jp

and Tebaldi (FT 1979),<sup>7</sup> where the period-doubling and the symmetry-breaking bifurcations are found but the quasi-periodic route is out of their result.

The Gledzer's original model of real variables  $v_i(t)$  for  $i = 1, \dots, n$  is given by:

$$\begin{aligned} \frac{dv_i}{dt} = \dot{v}_i = & c_{1,i}v_{i+1}v_{i+2} + c_{2,i}v_{i-1}v_{i+1} \\ & + c_{3,i}v_{i-1}v_{i-2} - \nu k_i^2 v_i + f_i, \end{aligned} \quad (1)$$

where  $v_i$  ( $f_i$ ) is the velocity (forcing) of the  $i$ -th mode in the space of a discretized wavenumber  $k_i$ .  $\nu$  denotes the kinematic viscosity, the forcing is assumed to be time independent, and  $v_0 = v_{-1} = v_{n+1} = v_{n+2} = 0$ . In order to conserve the energy  $E = \sum_{i=1}^n v_i^2$  and the enstrophy  $\sum_{i=1}^n k_i^2 v_i^2$  in the case of  $\nu = f_i = 0$  as Gledzer (1973) required for the model to be analogous to the two-dimensional turbulence, the coefficients of the nonlinear terms  $c_{j,i}$  for  $j = 1, 2, 3$  and  $i = 1, \dots, n$  need to satisfy the following relations:

$$c_{2,i+1} = -\frac{k_{i+2}^2 - k_i^2}{k_{i+2}^2 - k_{i+1}^2} c_{1,i}, \quad (2)$$

$$c_{3,i+2} = -\frac{k_{i+1}^2 - k_i^2}{k_{i+1}^2 - k_{i+2}^2} c_{1,i}. \quad (3)$$

If the wavenumber and the nonlinear coefficient  $c_{1,i}$  are selected as  $k_i = c_{1,i} = k_0 q^i$ , the above relations become

$$c_{2,i} = -\beta k_{i-1}, \quad (4)$$

$$c_{3,i} = (\beta - 1)k_{i-2}, \quad (5)$$

where

$$\beta = 1 + q^{-2}. \quad (6)$$

However, we switch the parameters chosen by OY,  $\beta = 1/2$  and  $q = 2$  in (4), (5),  $k_i$  and  $c_{1,i}$ , which do not satisfy (6), modeling the 3D turbulence in the sense that the conservation law holds only for energy, not for enstrophy.

Assuming that the forces are applied only on the first and second modes  $f_1 = f_2 = 1$  and  $f_i = 0$  for  $i \geq 3$ , the equation for the total energy with the forcing and the viscosity becomes

$$\dot{E}/2 = f_1 v_1 + f_2 v_2 - \nu \sum_{i=1}^n k_i^2 v_i^2. \quad (7)$$

If we consider the sufficiently large values of  $v_i$  such that  $|v_i| > |f_i|/(\nu k_i^2)$  for the forced modes  $i = 1, 2$ , the right hand side becomes negative and the solution is proved to be finite. The present model deals with real variables and therefore it is possible to reduce the dimensions of the model to the half with the same extent of the wavenumber, compared with the GOY

model.

Letting  $k_0 = 2^{-4}$ , the model becomes

$$\begin{aligned} \dot{v}_i = & 2^{i-5}v_{i+1}v_{i+2} - 2^{i-7}v_{i-1}v_{i+1} \\ & - 2^{i-8}v_{i-1}v_{i-2} - \nu 4^{i-2}v_i + f_i. \end{aligned} \quad (8)$$

The present model possesses a single parameter  $\nu$ , changed between the range about  $5 \cdot 10^{-2}$ - $5 \cdot 10^{-3}$ . Three ways of giving the initial condition are considered in order to examine multiple stable states. Case (I) is the origin;  $v_i(0) = 0$ . Case (II) [or (III)] is the final computed values of the slightly smaller [or larger] value of the viscosity  $\nu$ .

The Linux version of Mathematica 5.1 is used for the main part of the numerical integration. According to the manual of Mathematica, the general-purpose ODE solver developed by Hindmarsh (1983)<sup>8</sup> is adopted in the *NDSolve* command. The numerical solution is constructed checking its local convergence up to the machine precision of order  $10^{-16}$ . The weakest point is that it consumes large memory. The number of the modes is fixed as  $n = 6$  in the main part of this study. The computer has 1GB memory, its CPU is AMD Athlon XP 2000+ and its operating system is Vine Linux 3.2. A Fortran program with the fourth-order Runge-Kutta scheme with a fixed time step is also coded to check the bifurcation diagram in Figure 2 and no inconsistency is found between results by Mathematica and Fortran.

The number  $N(n)$  of fixed points (FPs) of (8) including complex numbers are computed by Mathematica and shown as  $N(4) = 5$ ,  $N(5) = 9$ ,  $N(6) = 25$ ,  $N(7) = 29$ ,  $N(8) = 61$ ,  $N(9) = 129$  and  $N(10) = 177$ , but the number of real fixed points is only 5 for  $n = 4, 5$  and 3 for  $6 \leq n \leq 10$  at  $\nu = 10^{-2}$ .

Figure 1 shows the bifurcation structure of the FPs; the stable (unstable) FPs are denoted by thick (thin) curves. The Mathematica program is coded such that the number of modes is arbitrary. The fact that the bifurcation structure is quantitatively the same between  $n = 6$  and 8 suggests the sufficiency of the six-dimensional system in the region  $0.005 < \nu < 0.05$ . The number of stable FPs is 1 for  $\nu > 0.03983(3)$ ,  $0.03482 > \nu > 0.02059(5)$ ,  $0.01287 > \nu > 0.01202(5)$ , 2 for  $0.02058 > \nu > 0.01288(5)$  and 0 for  $0.03982 > \nu > 0.03483(3)$ ,  $0.01201 > \nu$ . The number of total FPs is shown in the above parenthesis; 3 for  $0.05 > \nu > 0.03483$ ,  $0.01167 > \nu > 0.00967$ , 5 for  $0.03482 > \nu > 0.01168$ ,  $0.00968 > \nu > 0.00791$ , 7 for  $0.00790 > \nu > 0.00355$  and 9 for  $0.00354 > \nu$ . There is a tendency that as  $\nu$  decreases, the number of real FPs increases.

Figure 2(a) shows the bifurcation diagram of attractors by plotting values of  $v_1$  at the local maxima of  $v_1$  ( $\dot{v}_1 = 0$  and  $\ddot{v}_1 < 0$ ) between  $t = 9 \cdot 10^3$  and  $10^4$ , actually computed by the interpolation of three adjacent points with the time interval  $dt = 0.01$ . The initial condition is Case (I). The curve in the center of Fig.2(a) is therefore due to the stable FP.

The parameter region including the stable doubly-periodic state is examined in detail using

the initial condition of Case (II) and (III). The stable doubly-periodic solutions are confirmed to be generated through the supercritical Hopf bifurcation at about  $\nu = 0.03834$  as shown in the enlarged Figure 2(b) and Figure 2(c). The doubly-periodic solutions coexist with the periodic solutions with period  $6T$ , on which the incomplete period-doubling bifurcation occurs as seen in Fig. 2(b). Here, the period  $mT$  means that the periodic solutions give  $m$  points on the present Poincaré plot. The torus breakdowns at about  $\nu = 0.03785$  where the  $6T$ -periodic solution is still stable. Fig. 2(c) shows that there are windows of frequency-locking, which is one of the remarkable features of the sine-circle map. According to the current resolution in Figure 2(d), the  $6T$ -periodic solution changes chaotic suddenly at about  $\nu = 0.03724$ , indicating the intermittency route.

The left side of the chaotic parameter region in Fig. 2(a) is enlarged in Figure 2(e). Periodic windows are also observed among the chaotic solutions. A sequence of period-doubling bifurcations (Feigenbaum 1978)<sup>9</sup> of orbits is also observed in Figure 2(f), although it is in fact a revival of the periodic solution from chaos since the horizontal axis denotes the viscosity and the inviscid limit  $\nu \rightarrow 0$  turns to the left in the Fig. 2(f). Numerically computed examples of attractors projected on the  $(v_1, v_2, v_3)$  space for various values of  $\nu$  are shown in Figure 3.

In order to examine the circle map of the quasi-periodic solution, the pair  $(\hat{v}_1^{(n)}, \hat{v}_1^{(n+1)})$  is considered, where  $\hat{v}_1^{(n)} = v_1^{(n)} - \langle v_1^{(n)} \rangle$ ,  $v_1^{(n)}$  is the  $n$ -th plotted value of  $v_1$  and  $\langle \cdot \rangle$  denotes the time average. The points lie on a closed curve in the Poincaré section, showing the evidence of the doubly-periodic torus motion in the original 6D space. Denoting the  $2\pi$ -normalized argument of  $\hat{v}_1^{(n)} + i\hat{v}_1^{(n+1)}$  by  $\theta_n$  ( $0 \leq \theta_n < 1$ ), the one-dimensional map  $\theta_{n+1} = f(\theta_n)$  can be constructed.

In many studies of the circle map, the sinusoidal function is considered, but strictly speaking, the function is likely to deviate from it in real chaos systems of ODEs. We seek an approximation of the circle map of the form

$$\theta_{n+1} = f(\theta_n) = \theta_n + \Omega + \sum_{j=1}^M \frac{K_j}{2\pi j} \sin[2\pi j(\theta_n - \theta_0^{(j)})], \quad \text{mod } 1 \quad (9)$$

by applying the *FindFit* command of Mathematica to the numerically obtained data of the Poincaré plot with  $M = 10$ . Figures 4(a-c) show the dependence of  $K_j$  ( $j = 1, \dots, M$ ) and  $\Omega$  on the viscosity parameter. We observe the nonvanishing values of  $K_2, K_4, K_6$  even at the onset of the stable torus; i.e. the second Hopf bifurcation.

The numerical computation of the rotation number  $\rho$  on the torus is also possible by counting the number  $N_d$  of the decrease of  $\theta_n$  due to the modulus 1 in Eq. (9). A naive numerical approximation is  $\rho = N_d/N$ , where  $N$  is the number of the total Poicaré plot, denoted by small dots in Figure 5. A more elaborate method uses the power spectrum of

$v_1(t)$ . Choosing the suitable pair of two frequencies giving the maximum of the spectrum, we can identify the rotation number, denoted by larger dots in Fig.5. These two results are in agreement within the resolution of the numerical computation. The qualitative similarity is observed with that of the sine-circle map, showing the monotonic decrease of  $\rho$  and the flat region, i.e. the evidence of the *incomplete* devil's staircase.<sup>10</sup> Since our system has only one parameter, we just need to imagine the situation that two parameters ( $\Omega, K$ ) in the sine-circle map are changing simultaneously, as shown in Figures 4.

In summary, the two different routes to chaos coexist in the single Gledzer's model of six real variables. As noted by E. Ott<sup>11</sup> on page 199, the quasi-periodic route to chaos does not necessarily imply the bifurcation from double periodicity directly to triple periodicity or chaos, so-called the Ruelle-Takens scenario. The study of the sine-circle map indicates that frequency-locking leads to periodic solutions, which may become chaos through the period-doubling route or the other ones like symmetry-breaking or intermittency. The author has tested the Langford<sup>12</sup> equation, well known to have torus attractors, and finds a similar scenario suggested by Ott.<sup>11</sup>

According to Figures 4 and 12 in OY,<sup>2</sup> 10 positive Lyapunov exponents have been found for the 48-dimensional model of 24 complex variables and the dimension of the corresponding attractor should be very large. Their parameters  $\nu = 10^{-8}$  and  $f = (1 + i) \times 5 \times 10^{-3}$  correspond to the normalized viscosity  $\nu' = \nu/\text{Re}f = 2 \times 10^{-6}$  in our model with  $f = 1$ . Their computation time  $t = 400$  leads to the normalized time  $t' = (\text{Re}f)t = 2$  in our case with  $n = 6$ . The computation of Lyapunov exponents of our model, as well as motions of eigenvalues of the Jacobian, have been made but is not shown in this Letter. The triply-periodic motion has not yet identified in our model. It is still open whether the low-dimensional chaos shown in this study is connected or not with the state of turbulence which is considered to be independent of the parameter  $\nu$ , as we increase the number of  $n$  and decrease  $\nu$ . From the viewpoint of the bifurcation, it requires careful analysis but the gap will be filled as the power of the computer increases.

The author is grateful to Prof. T. Yamagata for encouragement, to Prof. H. Sakai for permission to use the file server, to Prof. W. F. Langford for sending me the related reprints on the Langford equation, and to Prof. L. Biferale for letting the author know his work before proofreading.

Figure 1. Bifurcation diagram of the fixed points (FPs) between  $5 \cdot 10^{-2} > \nu > 5 \cdot 10^{-3}$ . Stable (unstable) FPs are shown by thick (thin) curves.

Figure 2. Bifurcation diagram of attractors shown by values  $v_1$  at the local maxima of  $v_1$  ( $\dot{v}_1 = 0$  and  $\ddot{v}_1 < 0$ ).

(a) The range of the parameter  $\nu$  around  $5 \cdot 10^{-2} - 5 \cdot 10^{-3}$  and the initial condition is the origin.

(b) The parameter is  $0.0372 < \nu < 0.0409$  and the initial condition is Case(II) and (III) such that the multiple stable states of the double periodicity and the  $6T$ -periodicity are clearly captured. 20000 points are selected randomly for minute drawing.

(c) The enlarged Figure of (b) at  $0.0378 < \nu < 0.03834$  showing the second supercritical Hopf bifurcation, the doubly-periodic and frequency-locked periodic solutions (especially, 11:9, 17:14, 23:19 and 29:24 resonance), in addition to another stable  $6T$ -periodic solution.

(d) The parameter is  $0.0372 < \nu < 0.0384$ . The chaotic solution emerges suddenly at about  $\nu = 0.03724$ , indicating the intermittency route.

(e) Chaotic attractors with periodic windows at  $0.006 < \nu < 0.012$ .

(f) The enlarged figure of (e) at  $0.006734 < \nu < 0.00674$ , showing the evidence of the period-doubling bifurcation.

Figure 3. Projections of attractors on the  $(v_1, v_2, v_3)$  space at  $\nu =$  (a) 0.0395, (b) 0.0379, (c) 0.0378, (d) 0.037, (e) 0.0355, (f) 0.0118, (g) 0.0103, (h) 0.00883, (i) 0.0076, (j) 0.0074, (k) 0.0064 and (l) 0.006. (a) and (l) are the periodic solution of the period  $T$ , (k)  $2T$ , (f)  $3T$ , (h)  $4T$  and (g), (c)  $6T$ . (b) is the doubly periodic and (d), (j) are the chaotic solutions, respectively. (e) appears to be close to the heteroclinic orbit.

Figure 4. The dependence of the parameters in the circle map  $K_i$  with even  $i$  (a), odd  $i$  (b) and  $\Omega$  (c) on the viscosity  $\nu$ .

Figure 5. The numerically obtained dependence of the rotation number  $\rho$  on the viscosity  $\nu$ . The small (large) dots denote  $\rho$  by the method counting the number of decrease of  $\theta_n$  due to the modulus (computing the ratio of two frequencies giving the maximum of the power spectra of  $v_1$ ).

**References**

- 1) E. B. Gledzer: Sov. Phys. -Dokl. **18** (1973) 216.
- 2) K. Ohkitani and M. Yamada: Prog. Theor. Phys. **81** (1989) 329.
- 3) U. Frisch: *Turbulence* (Cambridge University Press 1995)
- 4) S. Kato and M. Yamada: Phys. Rev. E **68** (2003) 025302.
- 5) L. Biferale: Ann. Rev. Fluid Mech. **35** (2003) 441.
- 6) L. Biferale, A. Lambert, R. Lima, and G. Paladin: Physica D **80** (1995) 105.
- 7) V. Franceschini and C. Tebaldi: J. Stat. Phys. **21** (1979) 707.
- 8) A. C. Hindmarsh: Scientific Computing **8** (1983) 55.
- 9) M. J. Feigenbaum: J. Stat. Phys. **19** (1978) 25.
- 10) M. H. Jensen, P. Bak and T. Bohr: Phys. Rev. A **30** (1984) 1960.
- 11) E. Ott: *Chaos in Dynamical Systems* (Cambridge University Press 1993) 199.
- 12) W. F. Langford: *Nonlinear Dynamics and Turbulence* (Pitman Advanced Publishing Program 1983) 215.

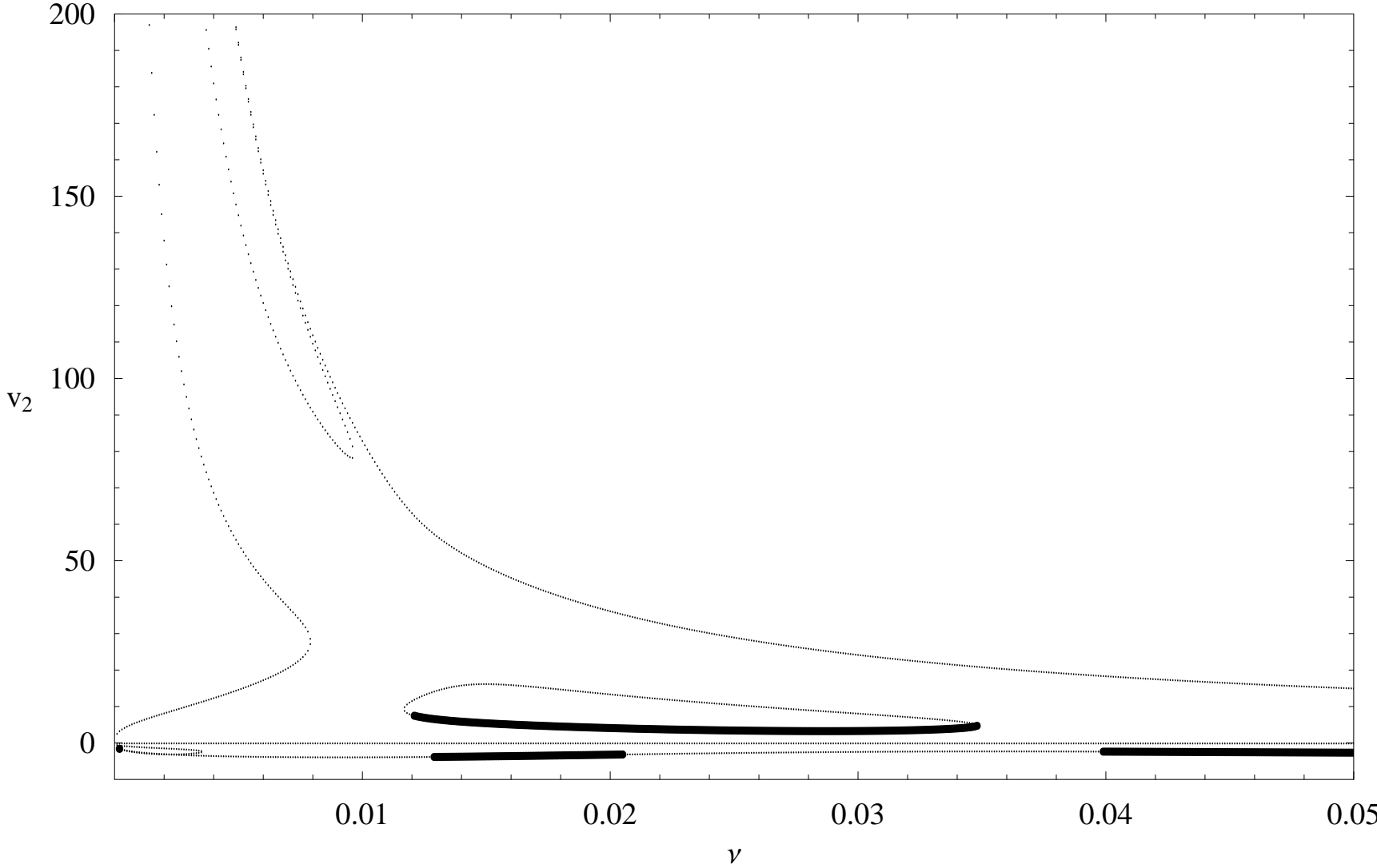


Figure 1

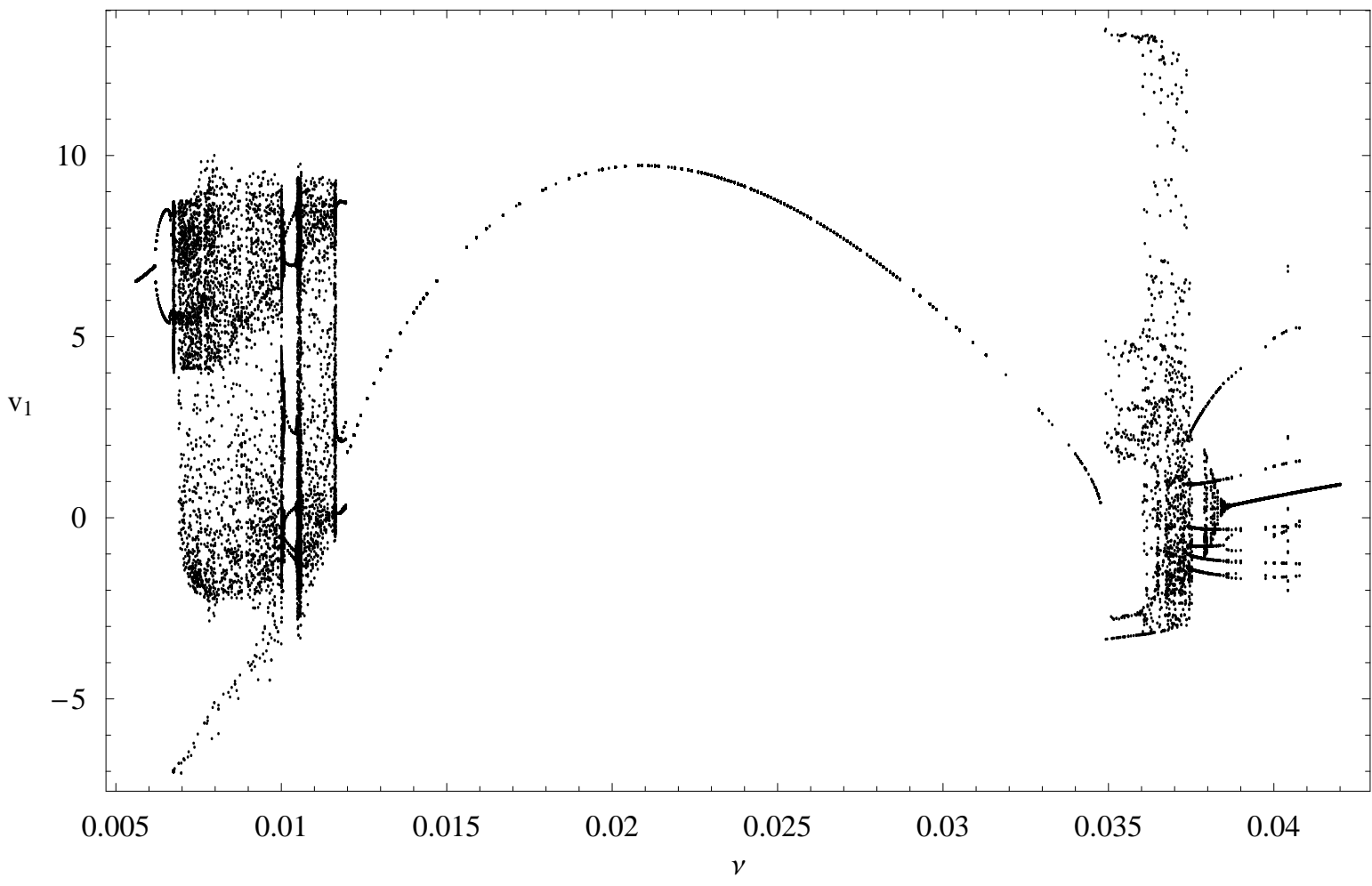


Figure 2a

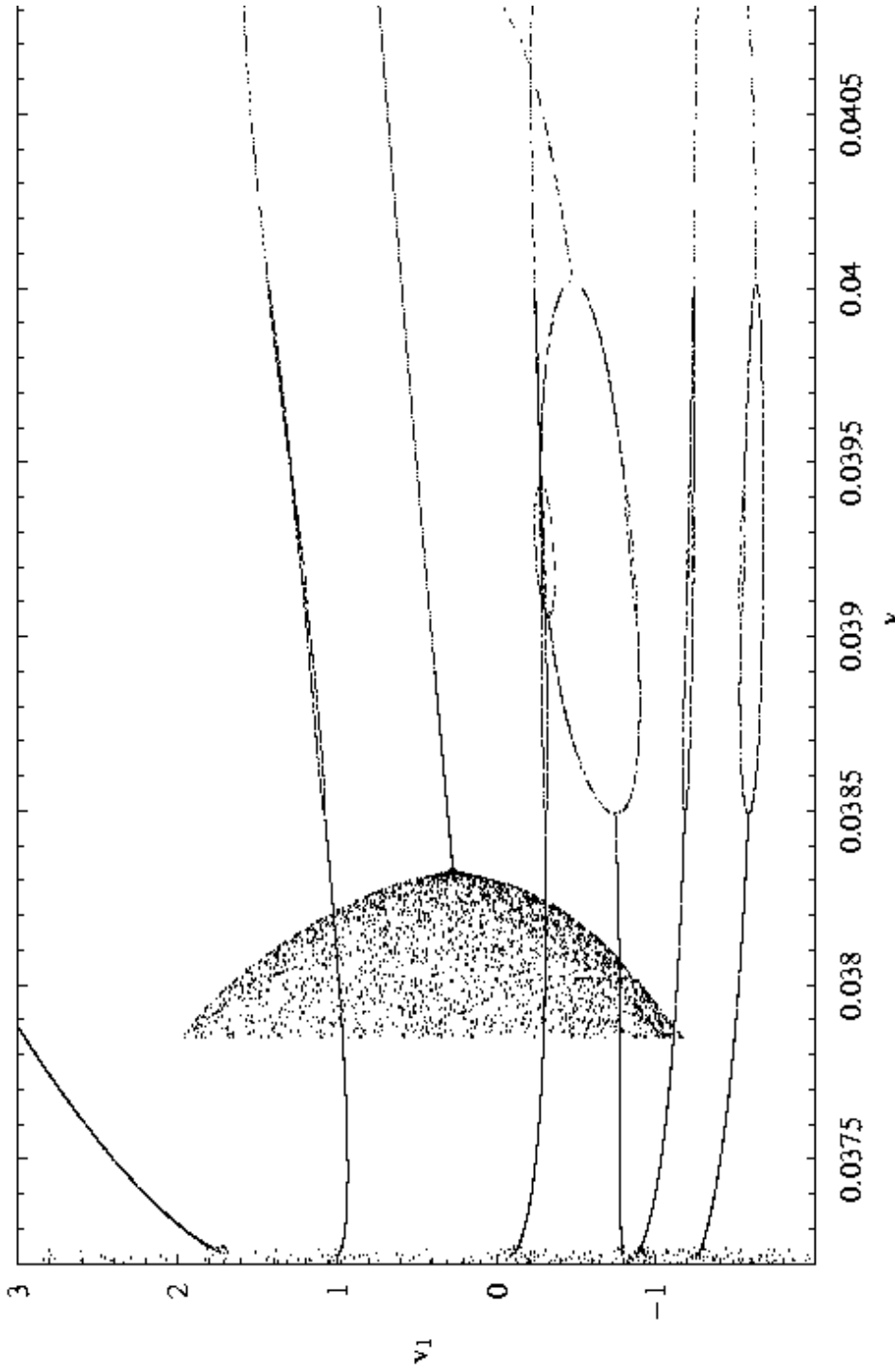


Figure 2b

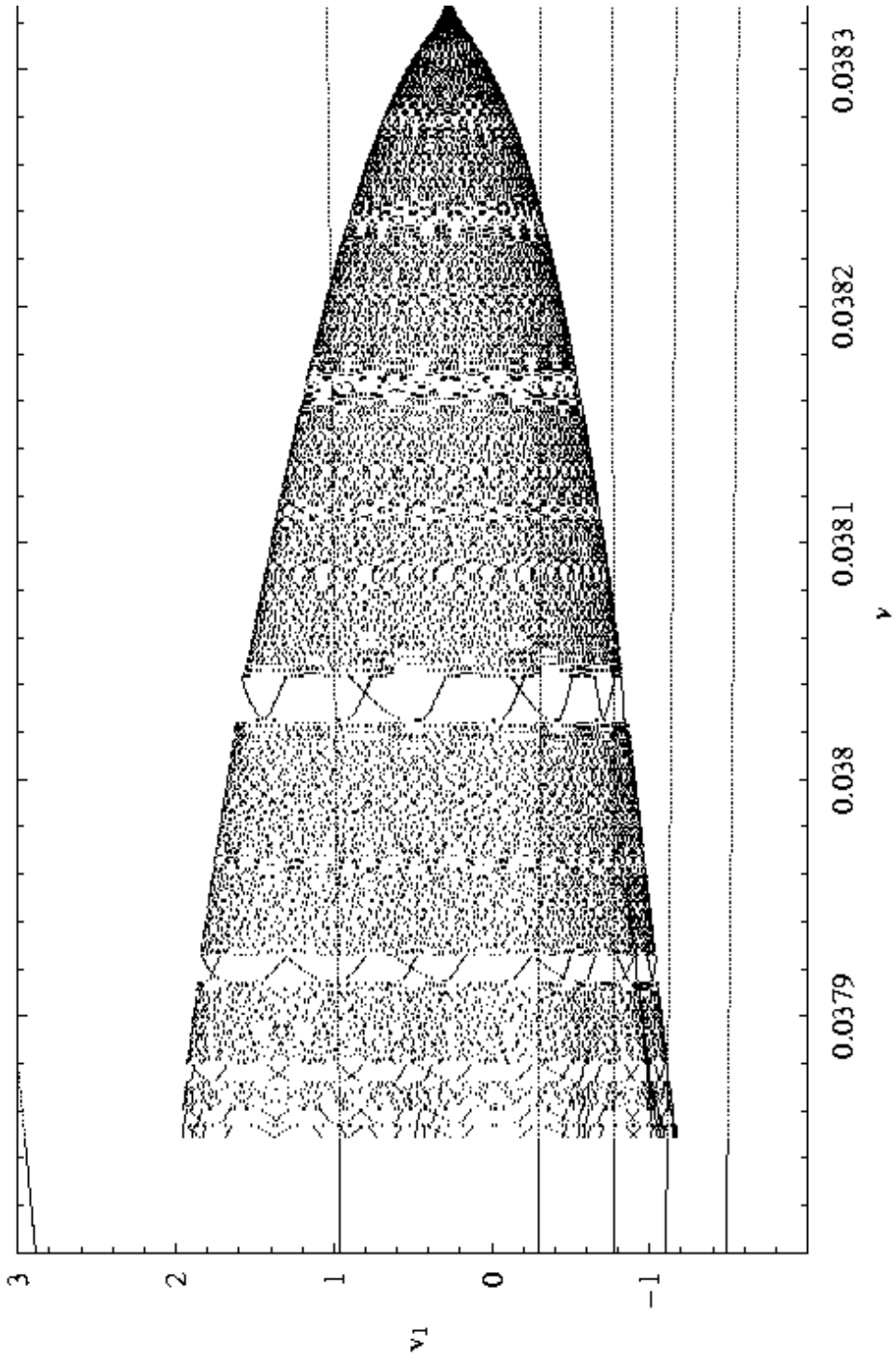


Figure 2c

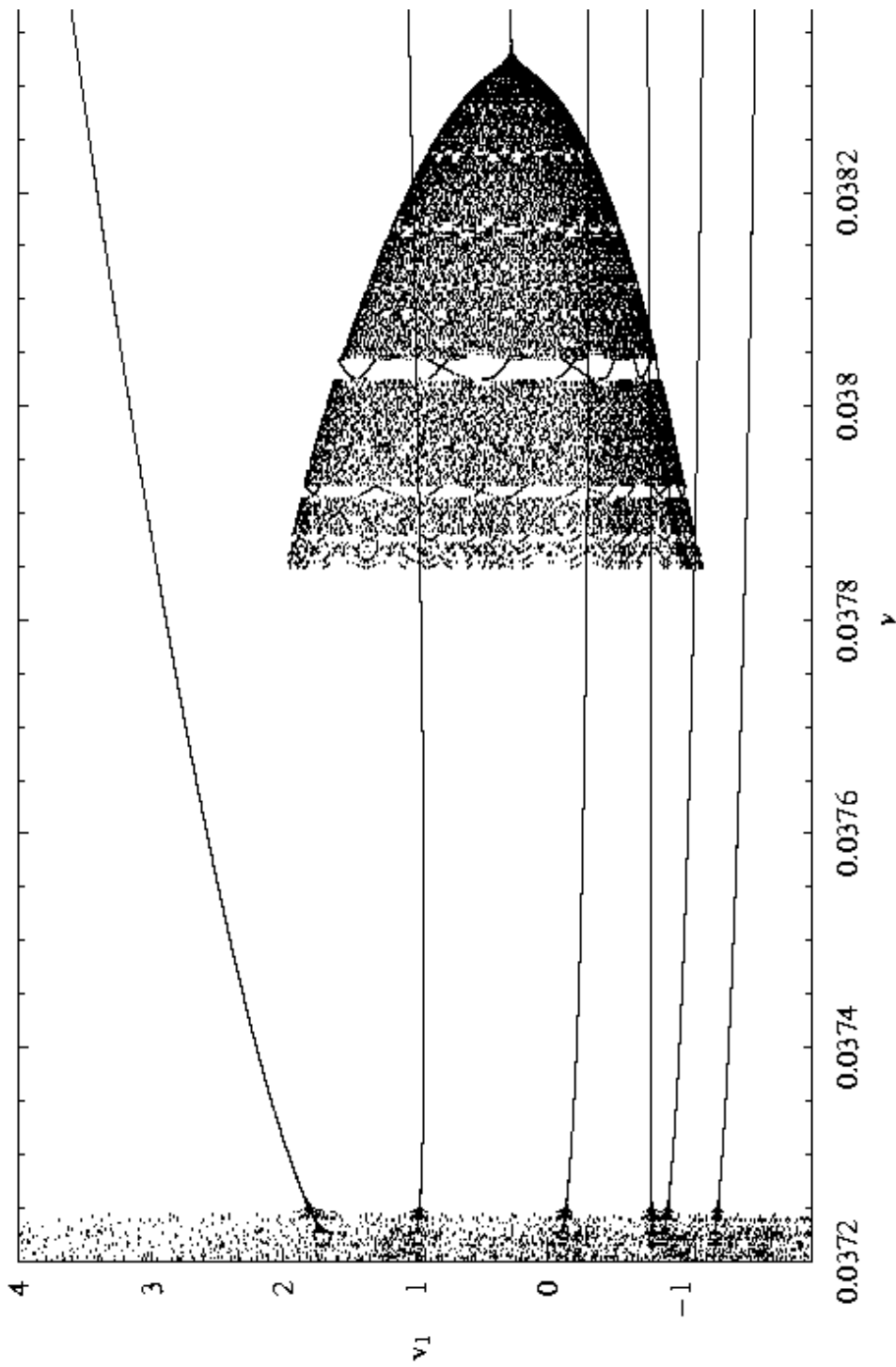


Figure 2d

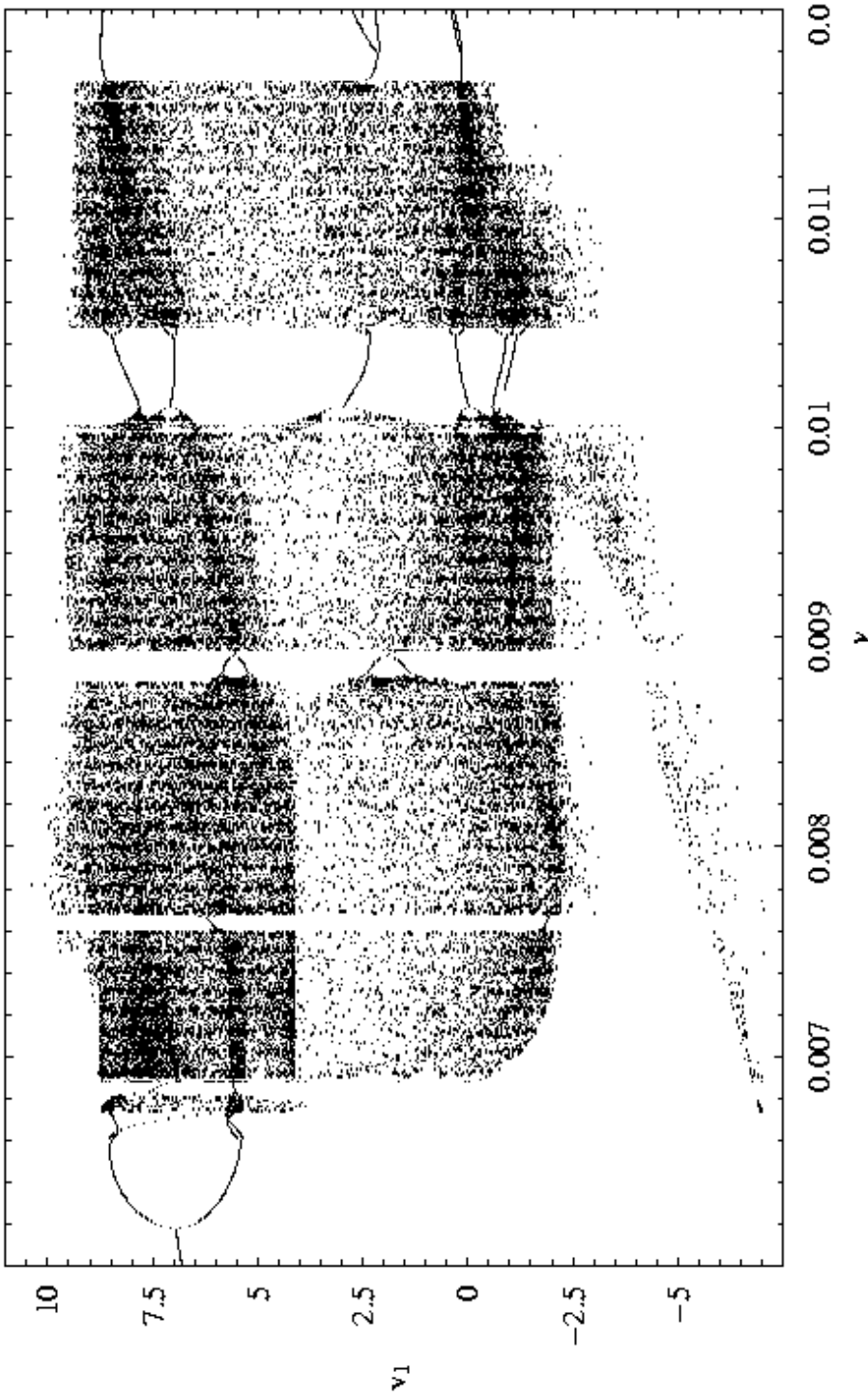


Figure 2e

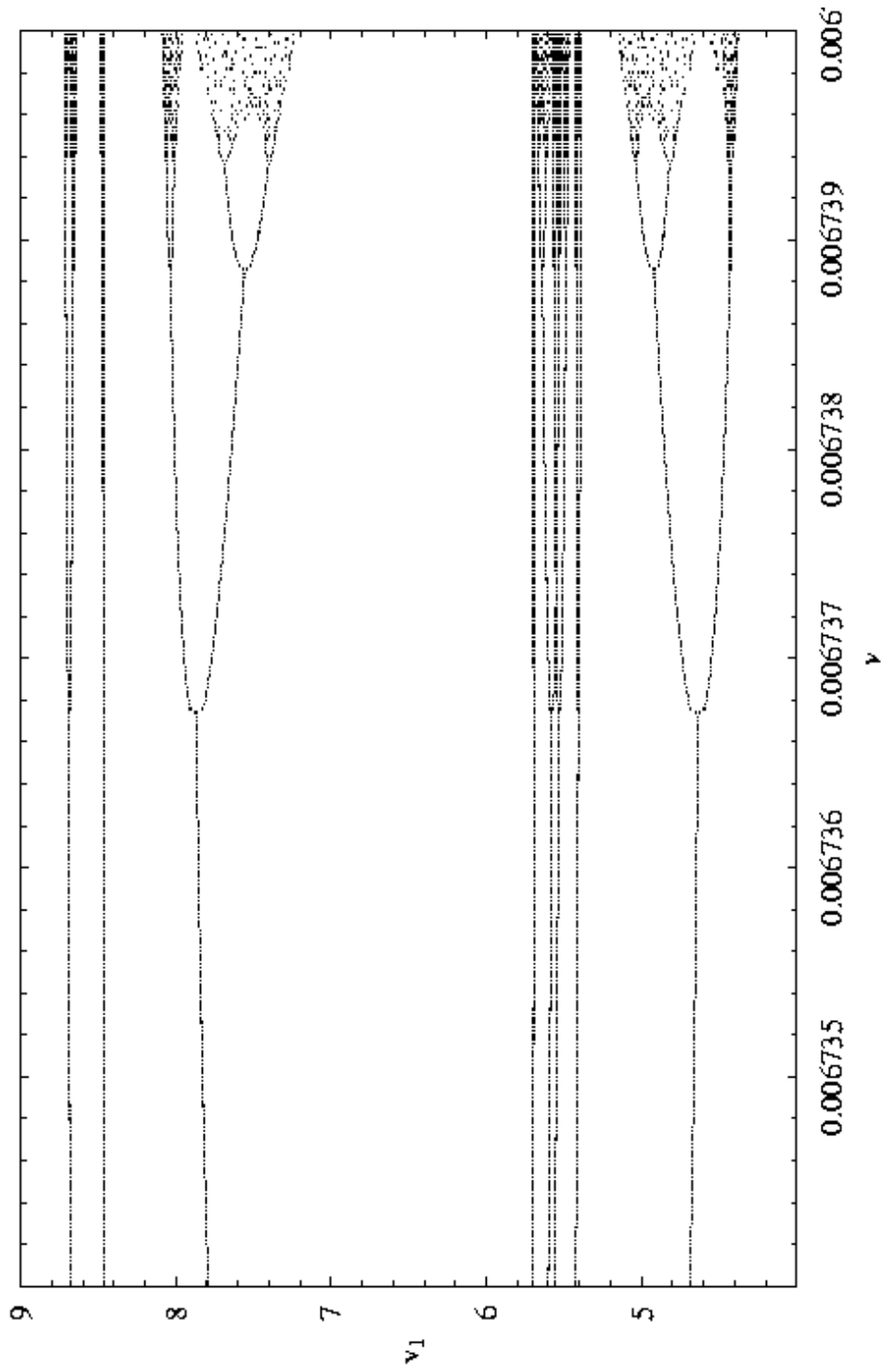


Figure 2f

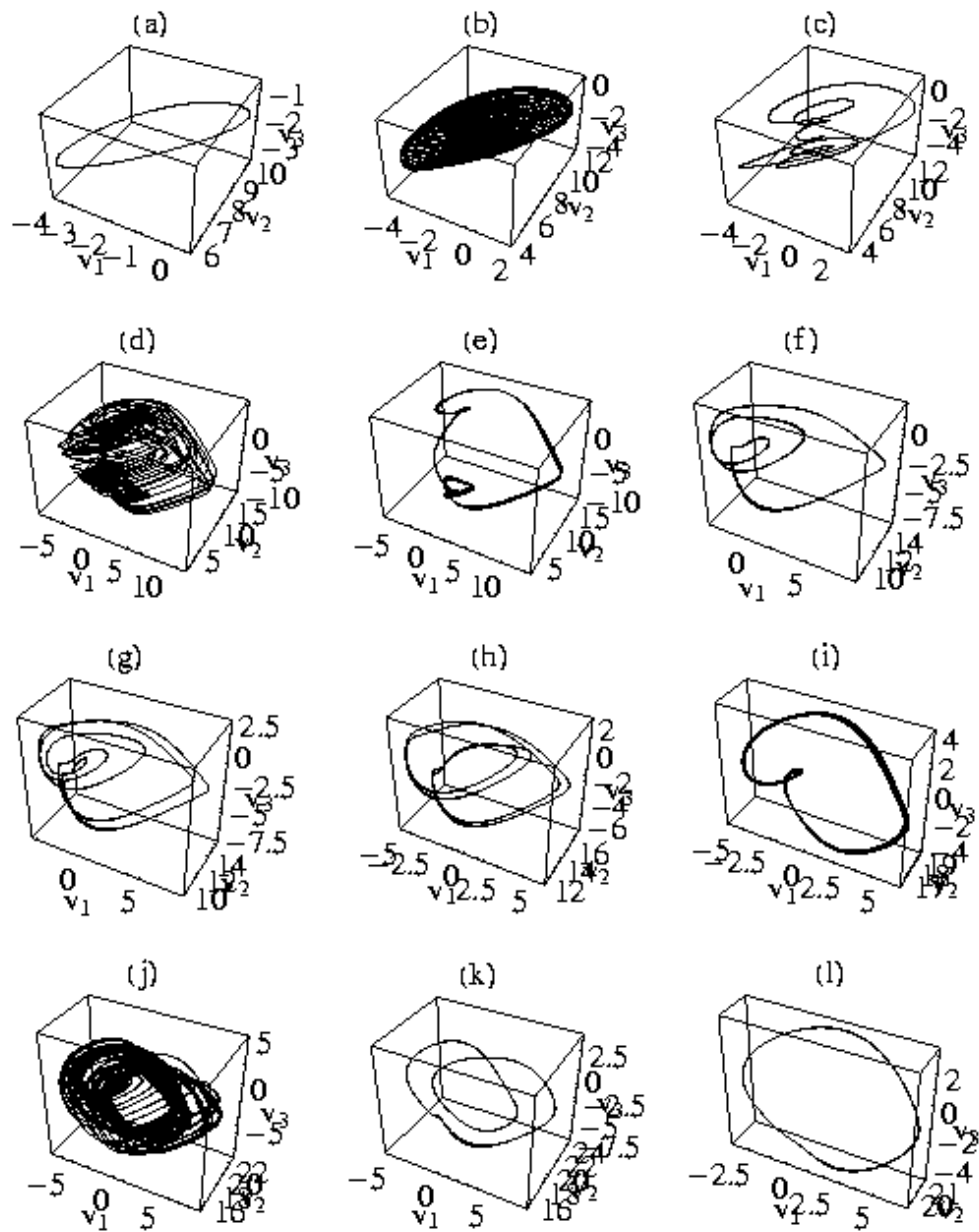


Figure 3

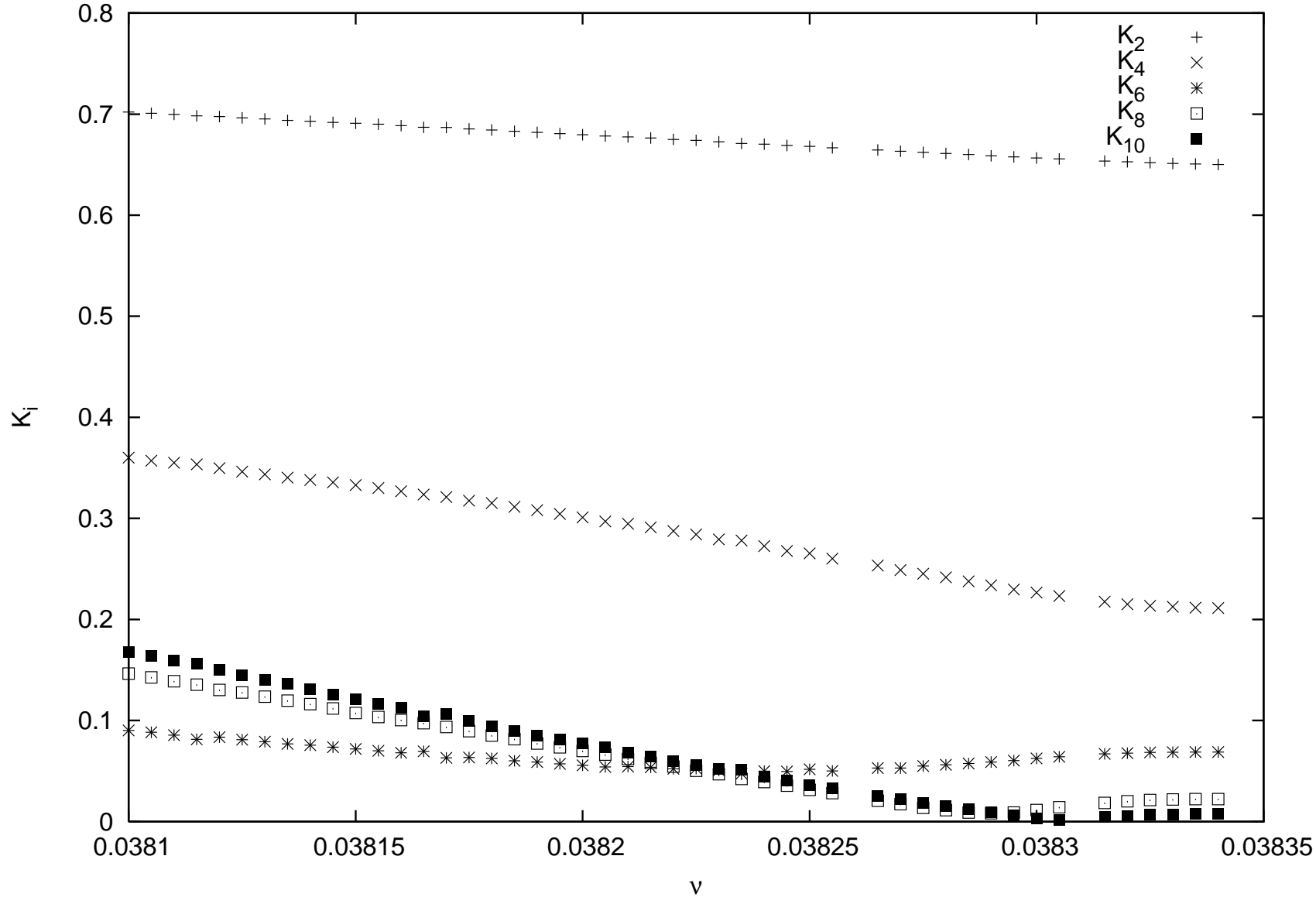


Figure 4a

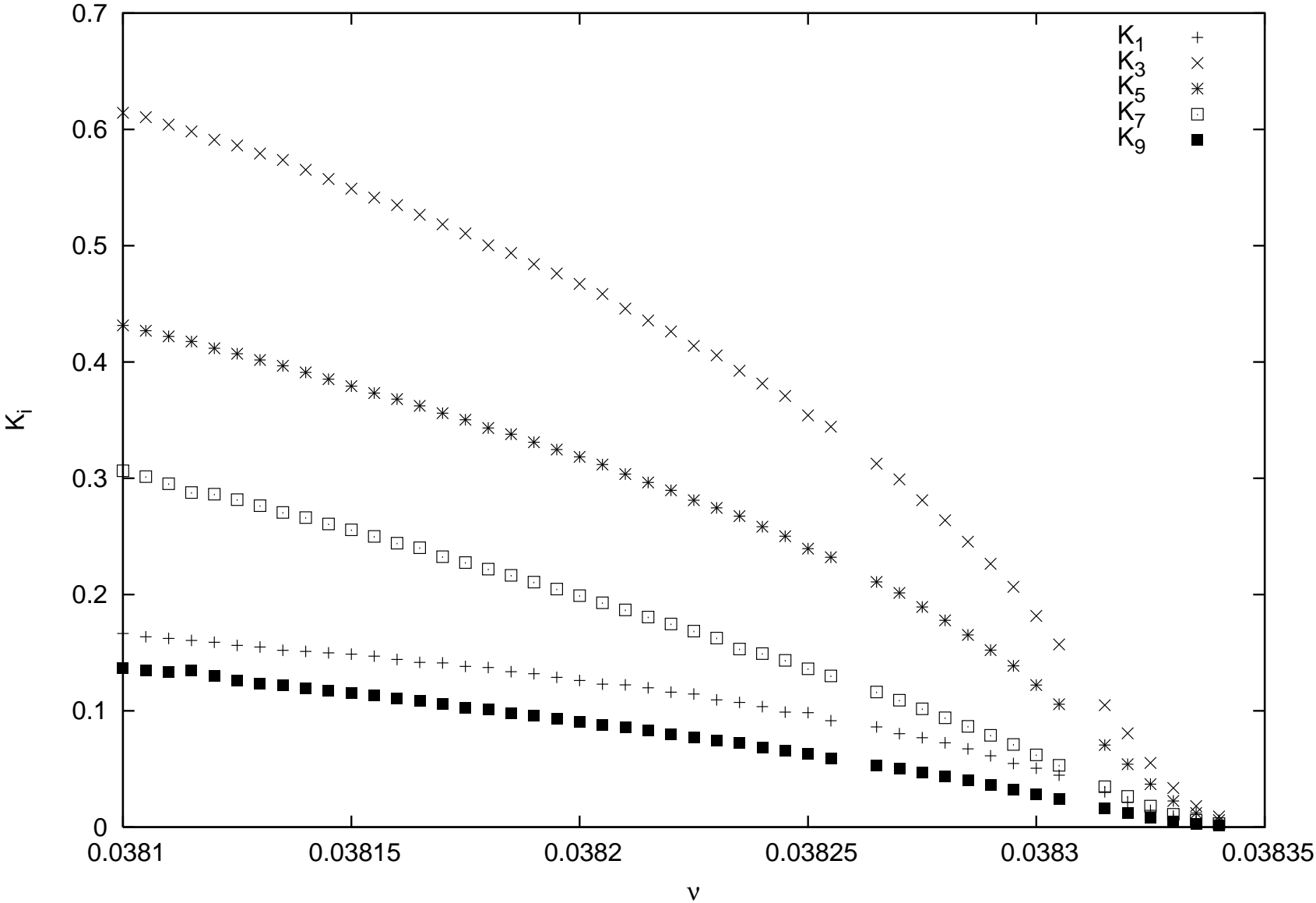


Figure 4b

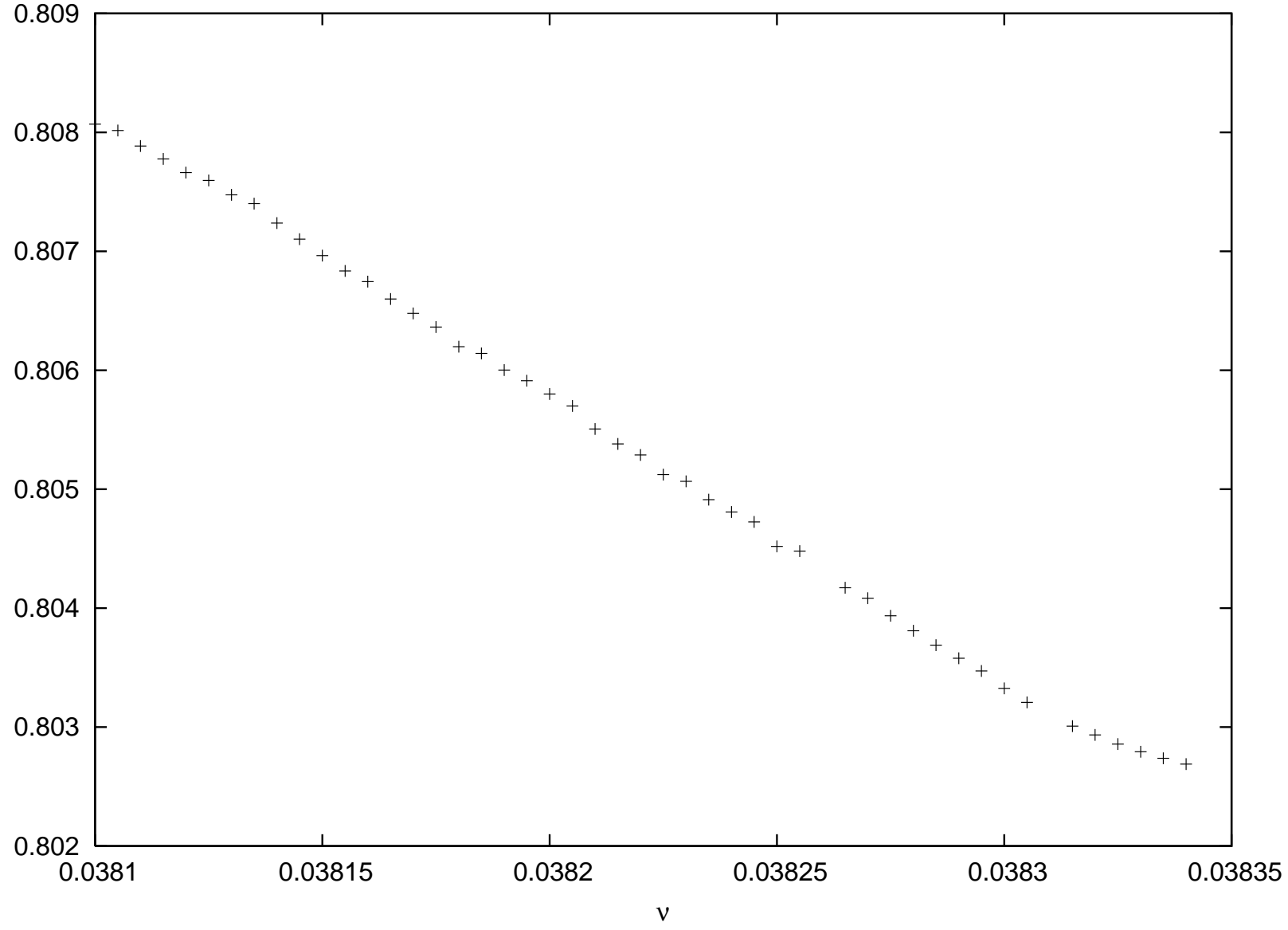


Figure 4c

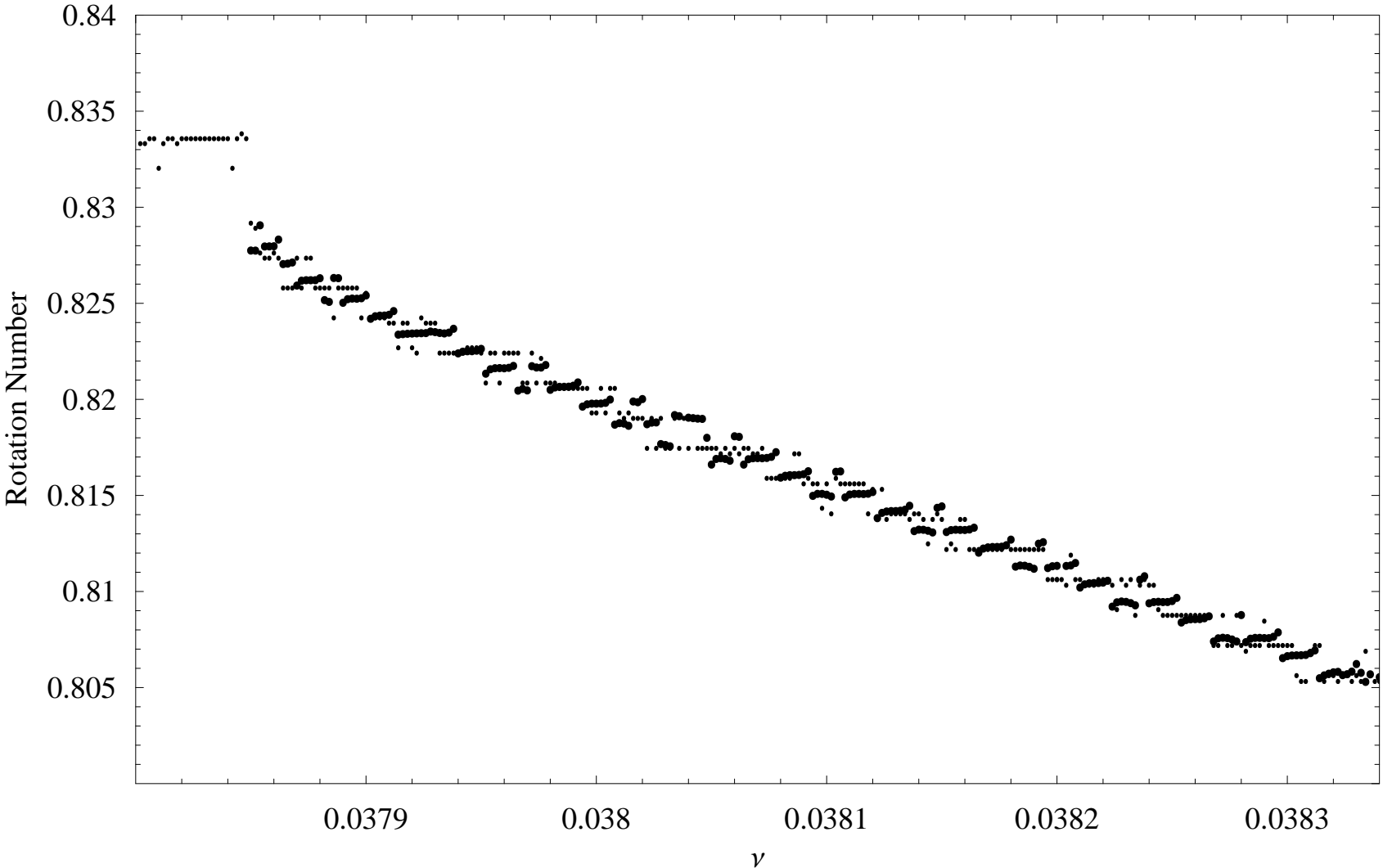


Figure 5